*Desalination and Water Treatment*
www.deswater.com
doi: 10.5004/dwt.2021.27756

238 (2021) 67–81
October

# Mechanical trajectory control of water mineral impurities in the electrochemical-magnetic reactor

Maziar Naderi[a], Simin Nasseri[a,b,*], Amir Hossein Mahvi[a,c], Alireza Mesdaghinia[a], Kazem Naddafi[a,d]

[a]*Department of Environmental Health Engineering, School of Public Health, Tehran University of Medical Sciences, Tehran, Iran, emails: maziar.naderi@gmail.com (M. Naderi), mesdaghinia@sina.tums.ac.ir (A. Mesdaghinia)*
[b]*Center for Water Quality Research (CWQR), Institute for Environmental Health Research (IER), Tehran University of Medical Sciences, Tehran, Iran, email: naserise@tums.ac.ir*
[c]*Center for Solid Waste Research, Institute for Environmental Research, Tehran University of Medical Sciences, Tehran, Iran, email: ahmahvi@yahoo.com*
[d]*Center for Air Pollution Research (CAPR), Institute for Environmental Research (IER), Tehran University of Medical Sciences, Tehran, Iran, email: knadafi@tums.ac.ir*

Received 2 April 2021; Accepted 19 August 2021

**ABSTRACT**

The paper is focused on the study of controlling the path of ions causing hardness and salinity of water by a combination of electrolysis process and electric and magnetic fields and explaining the mechanism of the process based on magnetohydrodynamic (MHD) and magnetophoretic (MP) forces. The results showed that the highest removal efficiency of total dissolved solids (TDS) was 7.64%, the highest removal efficiency of electrical conductivity (EC) was 38.32% and the highest removal efficiency of total hardness (TH) was 36.04%. The greatest impact occurred when these two forces were applied simultaneously. Moreover, $MgSO_4$ and $CaCO_3$ had the greatest effect on the reduction of ions. This effect was due to the presence of oxygen atoms of $MgSO_4$. Oxygen atoms are considered to be strong paramagnetic particles (magnetic susceptibility of $+7{,}699 \times 10^{-6}$ $m^3$/mol) due to their unpaired orbitals, which makes them more affected. Besides, the ions that increase the TDS and EC of water (such as NaCl and $MgSO_4$) have a larger rotation diameter or Larmore radius than ions that increase water TH. The circulation of soluble ions around the central electrode was formed by the MHD force that was based on the Lorentz force, and the difference in the concentration of ions in the column was caused by the MP force that was based on the Kelvin force and as a result, more ions were transferred to the spiral paths.

*Keywords:* Mechanical trajectory; Mineral impurities; Magnetohydrodynamic force; Magnetophoretic force; Larmore radius; Lorentz force; Kelvin force

## 1. Introduction

Desalination is the process of removing excess salts and other dissolved minerals from the seawater that reduces salt concentrations at or below the World Health Organization's drinking water limit of 500 mg/L [1,2]. Brine is the concentrated stream of the desalination process that has an adverse impact on the environment. Hence, cost-effective brine stream management methods are needed to reduce environmental pollution [3]. At present, various disposal methods have been used, including surface water discharge, sewer discharge, deep-well

* Corresponding author.

injection, evaporation ponds and land applications [3]. However, these brine disposal methods are unsuitable and are limited by high capital costs and non-global application [3]. The most important parameters considered in such concentrated flows are salinity and hardness. Salinity can make water non-drinkable and damage aquatic life [4]. Moreover, the presence of high hardness in water causes the formation of sediments in water facilities and reduces operating costs [5]. Brine treatment is considered one of the most promising alternatives to brine disposal [3]. Chemical treatment is the main method used in brine treatment to reduce and remove water minerals. This method is costly and not environmentally friendly [6]. Therefore, it is necessary to provide an effective method of water treatment that is low cost and at the same time creates minimal environmental pollution [7]. Physical water treatment systems include magnetic, electrostatic, ultrasonic and hydrodynamic processes [8]. Magnetism is a unique physical property that independently helps in water treatment by influencing the physical properties of impurities in water. The contact of water with magnetic fields causes many phenomena in water, even if the magnetic field intensity is weak and the contact time is short [9]. Many researchers believe that magnetic water treatment is one of the most effective non-chemical methods [6]. Han et al. [10] investigated the influence of alternating electromagnetic fields and ultrasonic on calcium carbonate crystallization in the presence of magnesium ions. The effects of magnetic and electric fields on physicochemical properties of water have been the most controversial field for at least 50–60 y [11,12]. In water treatment by electric forces, an electric field is applied around the water that has metal electrodes. In magnetic systems, a coil is placed around the water pipe and a magnetic field is applied to the water [8]. Although these methods have not been specifically used on a commercial scale, they have been considered as pretreatments in membrane processes [13]. This process incorporates a set of electrochemical, magnetic, and hydrodynamic concepts. The interaction of the magnetic field with the current density causes water to rotate around the electrode, which is called the magnetohydrodynamic effect (MHD) and occurs in uniform magnetic fields [14]. The origin of this rotational force is the driving force of electric motors known as Lorentz force. In this process, the electrodes are placed in water and an external magnetic field is applied to the system [13]. Most recent studies in the field of magneto-electrochemistry have been devoted to the study of the effect of Lorentz force on the rotational current in an electrochemical cell [14]. Gatard et al. evaluated the use of magnetic fields in electrochemistry [15]. MHD effects involving the interaction of the magnetic field with the local electric current density are the contained mechanism in the process [13]. In the process also a force is applied directly on paramagnetic species in the electrolyte that is named magnetophoretic (MP) or Kelvin force [14]. The force is due to the gradient concentration of paramagnetic ions. Besides, the electromagnetic force is the other force acting on electric currents [13]. Both types of force are usually present, because any redox process where a single electron is transferred necessarily involves paramagnetic species, but one or the other is often dominant [14]. A study on the effects of magnetic field gradients on paramagnetic free radicals in solution was stimulated by White [16]. The interaction creates local paramagnetic concentration gradients and induces convection near an electrode [13]. MHD is the study of the flow of electrically conducting liquids in electric and magnetic fields [17]. The equations of the MHD principles come from two parts, classical fluid dynamics and electromagnetics [18]. The former includes mass continuity equation and Navier–Stokes equation and the latter include Maxwell's equations, current continuity equation and constitutive equations [17]. Recent progress in MHD has gone beyond a study of the influence of the Lorentz force on convection on different length scales. Attention is turning to non-uniform fields, and the Kelvin force, which can be very large at ferromagnetic electrodes. Monzon and Coey [13] studied the magnetic fields in electrochemistry and focused on the electromagnetic forces acting on electric currents. They showed that the Lorentz force was the predominant mechanism in magneto-electric interaction. Monzon and Coey [14] also surveyed the influence of magnetic field gradients on paramagnetic species in an electrochemical cell and explained the mechanism based on the Kelvin force. In another study, Terentiev et al. [19] also carried out a study on the electromagnetic effects of water impurities. They have controlled the mechanical trajectory of impurities by a magneto-electric device using the combination of the Lorentz force and the Larmore force and removed them from the main flow. Although the influence of an applied magnetic field on the operation of an electrochemical cell has been studied for over 40 y, MHD remains relatively unfamiliar territory to all but a few specialized research groups [20]. The topic is concepts from electrochemistry, hydrodynamics and magnetism. Magnetic water purification is an attractive method, but it still raises controversial issues and its phenomena cannot be clearly explained. Regarding increasing demand for drinking water and a decrease in freshwater resources, the use of membrane technology is a common approach. One of the disadvantages of this treatment method is the production of a concentrated stream containing high hardness and salinity. In recent years, the use of physical methods such as the use of magnetic and electrical forces to water treatment in terms of mineral depletion has significantly increased. However, in the methods magnetic and electrical forces have been separately studied. Besides, these forces have been used to prevent the deposition of water mineral components and also to change the structure of sediments. In the method presented in this study, magnetic and electric forces were applied simultaneously in a reactor in order to deflect the minerals of water. This method is a new deionization technique in the field of magnetic-electric water purification, and the optimization of this system based on the physical parameters of the reactor has not been carried out in previous studies. Magnetic treatment is a technique that has been separately applied to dissolved chemicals in the water. In this research, magnetic and electric forces were used simultaneously in a reactor to deflect the magnetic particles of water. The purpose of this study was to present a physical method for the separation of hardness and salinity agents by magnetic and electrical forces.

## 2. Materials and methods

### 2.1. Design and construction of the electrochemical-magnetic system

The designed system had a glass cylinder with a diameter of 5 cm, in the upper part of which two graphite anode and cathode electrodes were placed opposite each other to separate cations and anions. The potential difference between these electrodes was considered to be 0.5–1 V, which was supplied from a DC power supply. This potential difference was considered to prevent the occurrence of the electrolysis process. In addition, two permanent neodymium magnets (with a magnetic field strength of 0.18 around the tube and 0.05 T in the center of the tube) were placed around the electrodes so that the magnetic field lines were perpendicular to the direction of electric charge movement of the two electrodes. The applied magnetic field causes the ions to better separate from each other. In the center of the column, a steel cathode electrode was placed to guide the ions to the center tube. The voltage applied to the central electrode was also supplied by a DC variable power supply. In the middle of the tube, a coil was designed to produce a non-uniform magnetic field around the column. The height of the coil was 10 cm and the number of turns of the coil was 1,500 turns. The magnetic flux density generated in water was calculated using the following equation:

$$B = \frac{\mu_0 NI}{L} \quad (1)$$

where $\mu_0$ is the vacuum permeability coefficient, $N$ is the number of turns of the coil, $I$ is the intensity of the electric current and $L$ is the length of the coil. In this study, the water permeability coefficient is used instead of the vacuum permeability coefficient. The magnetic permeability constant of water is $1.256627 \times 10^{-6}$. By changing the current intensity of the coil (0.55, 2.22, 3.88, 5.55 and 7.22 Å), the different magnetic flux densities of 0.01, 0.04, 0.07, 0.1 and 0.13 T were created, respectively. DC power supply with an adjustable electrical voltage of 0–30 V and a current intensity of 0–10 A (Dazheng Co., China) was used for magnetic fields generation. To drain the condensed water, a tube with adjustable diameters of 0.1, 1, 1.5, 2 and 2.5 cm was installed at the bottom of the central electrode. Distances of 1.5, 2, 2.5, 3 and 3.5 cm from the central electrode to the central tube were studied. At the end of the column, two valves were disconnected and connected to remove desalinated water and condensed water from the column, as well as to adjust the flow rate of the outlet flows. The intended water flow rates in this study were 2, 4, 6, 8, and 10 mL/s. The electrochemical-magnetic reactor is depicted in Fig. 1.

### 2.2. Preparation of electrolyte solutions

To prepare the electrolyte solutions, NaCl, $CaCO_3$ and $MgSO_4$ salts were used in different proportions. The NaCl electrolytes were prepared by sodium chloride salt with a purity of 99.5% (Merck Company, Frankfurter Str. 250, 64293 Darmstadt, Germany) at the concentrations of 0.5, 1, 1.5, 2 and 2.5 g/L. The $CaCO_3$ electrolytes were prepared by $CaCO_3$ salt with a purity of 99.5% (Merck Company, Frankfurter Str. 250, 64293 Darmstadt, Germany) at the concentrations of 0.1, 0.2, 0.3, 0.4 and 0.5 mg/L. The $MgSO_4$ electrolytes were prepared by $MgSO_4$ salt with a purity of 99.5% (Merck Company, Frankfurter Str. 250, 64293 Darmstadt, Germany) at the concentrations of 0.1, 0.2, 0.3, 0.4 and 0.5 g/L.

### 2.3. Experimental design

To determine the number of experiments and statistical analysis of data, experimental design (ED) and response surface methodology (RSM) were used. Experimental design of the system was carried out using central composite design (CCD) methodology. The CCD is widely used for the RSM. The design was conducted in 5 blocks. RSM is a collection of mathematical and statistical methods for the modeling and analysis of a process in which a response of interest can be influenced by several variables. Indeed, it is used to determine the optimum operating conditions or

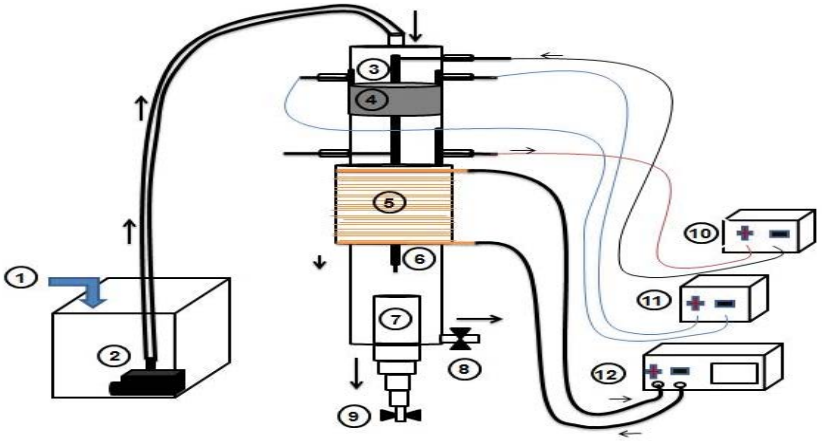


Fig. 1. Schematic diagram of the electrochemical-magnetic reactor for chlorine gas production: (1) sample inlet; (2) submerged pump; (3) peripheral graphite electrodes; (4) neodymium magnet; (5) coil; (6) central steel electrode; (7) central drainage tube; (8) deionized outlet water; (9) concentrated outlet water; (10)–(12) DC power supply.

to determine a region for the factors in which certain speciation are met. The CCD was used to describe the process in the experimental domain and also for the optimization of this process to have the best reduction in total dissolved solids (TDS), electrical conductivity (EC) and total hardness (TH). This design is formed by uniformly distributed points within the space of the coded variable ($X_i$). One of the advantages of CCD is the possibility to explore the entire experimental region and the usefulness of interpolating the response. For the axial runs matrix, α has been chosen in order to have iso-variance property by using rotation. The experimental response associated with a CCD matrix is represented by a quadratic polynomial model [21]:

$$Y = b_0 + \sum_{i=1}^{k} b_i \cdot X_i + \sum_{i=1}^{k} b_{ii} \cdot X_i^2 + \sum_{j} \sum_{i=2}^{k} b_{ij} \cdot X_i X_j \quad (2)$$

where $Y$ experimental response; $b_0$ average of the experimental response; $b_i$ estimation of the principal effect of the factor $j$ for the response $Y$; $b_{ii}$ estimation of the second effect of factor $i$ for the response $Y$; $b_{ij}$ estimation of the interaction effect between factors $i$ and $j$ for the response $Y$.

The coefficients of this model are calculated in the experimental region using the least square method [22]:

$$B = \left(X^T X\right)^{-1} X^T Y \quad (3)$$

where $B$, vector of estimates of the coefficients; $X$, the model matrix; $Y$, the vector of the experiment results. A seven-factorial and a two-level CCD, with 12 replicate at the center point led to a total number of 154 experiments employed for response surface modeling. The independent process variables used in this study were: the NaCl concentration ($X_1$), $CaCO_3$ concentration ($X_2$), $MgSO_4$ concentration ($X_3$), flow rate ($X_4$), diameter ($X_5$), distance ($X_6$) and magnetic flux density ($X_7$). The experimental values of $U_i$ can be calculated from the coded variables $X_i$ using the following equation:

$$X_i = \frac{U_i U_{i,0}}{\Delta U_i} \quad (4)$$

where $U_{i,0} = (U_{i,\max} + U_{i,\min})/2$, represents the value of $U_i$ at the center of the experimental field; $\Delta U_i = (U_{i,\max} - U_{i,\min})/2$, represents the step of the variation, with $U_{i,\max}$ and $U_{i,\min}$ which are the maximum and minimum values of the effective variable $U_i$, respectively. Total hardness reduction ($Y_1$), total dissolved solids ($Y_2$) and electrical conductivity ($Y_3$) were considered as dependents factors (response). The values of process variables and their variation limits were selected based on the preliminary experiments. In studies where the number of variables is large, the design is done in more blocks. Each block is modeled separately in the form of a three-dimensional regression figure or RSM and its optimal point is determined. In each block, the different points of the variables are placed next to each other based on the multiplication of the positive and negative symbols of the code of the variables (+1 and –1). Experimental data were analyzed using R 3.6.2 program software including analysis of variance (ANOVA) in order to obtain the interactions between the process variables.

### 2.4. Reactor-related experiments

Various operating parameters, such as electrolyte concentration (NaCl, $CaCO_3$ and $MgSO_4$), water flow rate, central tube diameter, the distance between the tube with the central electrode and magnetic flux density were evaluated. The types of variables and their levels based on the CCD design have been shown in Table 1. In this design, 154 experiments were performed, which were designed in five blocks. The samples were poured into the storage tank and then pumped by the submerged pump inserted in the storage tank. A direct current (DC) is applied between the two electrodes above the column and the coil around the column. The current applied between the electrodes and the coil was DC. The column outlet valve was then adjusted based on the considered flow rate of each experiment. When water containing ions was pumped into the column after 5 min detention time for the electrolysis process and the formation of helical paths around the central electrode, the end valve of the column was opened to release concentrated water. Treated water was discharged through the peripheral side of the column, and a concentrated stream was discharged through the central tube. Furthermore, in order to influence the forces involved in this system, 3 experiments with 3 repetitions were performed (1) without MF force, (2) without MHD force, and (3) without MP and MHD forces.

### 2.5. Analytical experiments

TDS, EC and TH of the sample water entering the system and the water leaving the column were measured and the reduction efficiency of these parameters in different conditions was reported. TDS and EC were measured by a digital conductivity meter (HACH conductivity meter CDC 401, Hach Company, P.O. Box 389, Loveland, Colorado 80539-0389) and the removal efficiency of each parameter was calculated. Moreover, the total hardness of the input and output samples was measured by ethylenediaminetetraacetic acid (EDTA) titration. Water hardness is due to the presence of calcium and magnesium cations. Although other cations such as iron and manganese can also produce hardness, because their concentration in water is very low, the sum of calcium and magnesium cations is called water hardness. Water hardness is usually divided into temporary hardness and permanent hardness. Temporary hardness (or carbonate hardness) refers to the calcium and

Table 1
Experimental range and levels of independent factors

| Factor | Range and levels | | | | |
|---|---|---|---|---|---|
| | –α | –1 | 0 | 1 | +α |
| NaCl, mg/L | 0.5 | 1 | 1.5 | 2 | 2.5 |
| $CaCO_3$, mg/L | 0.1 | 0.2 | 0.3 | 0.4 | 0.5 |
| $MgSO_4$, mg/L | 0.1 | 0.2 | 0.3 | 0.4 | 0.5 |
| Flow rate, mL/s | 2 | 4 | 6 | 8 | 12 |
| Diameter, cm | 0.5 | 1 | 1.5 | 2 | 2.5 |
| Distance, cm | 1.5 | 2 | 2.5 | 3 | 3.5 |
| Magnetic field, T | 0.01 | 0.04 | 0.07 | 0.1 | 0.13 |

magnesium bicarbonate salts that become insoluble in solution when heated, as shown in the reaction below.

$$Ca(HCO_2)_2 \xrightarrow{Heat} CaCO_2 \downarrow H_2O + CO_2 \uparrow \quad (5)$$

Water hardness occurs mainly due to the presence of calcium and magnesium ions, both of which are easily chelated in the presence of the sodium salt of EDTA. Magnesium precipitates as $Mg(OH)_2$ at pH above 12 and calcium ions remain in solution. Therefore, at pH = 12–13, only the calcium ions in the sample combine with EDTA. At first, the Eriochrome™ Black T indicator (ECBT) was prepared. To prepare this indicator, 0.5 g of this reagent and 4.5 g of hydroxylamine hydrochloride were mixed and the resulting mixture was then dissolved in 100 mL of ethanol. In order to prepare the morxide indicator, dry morxide was primarily mixed with dry NaCl in a mortar in a ratio of 1:100 and 0.1 g of the mixture was dissolved in 100 mL of ethanol. To prepare the buffer at pH = 10, 57 mL of concentrated ammonia was added to 7 g of ammonium chloride and brought to a volume of 100 mL. Moreover, to prepare a standard solution of 0.1 M calcium, 1 g of anhydrous $CaCO_2$ was poured into humans and 5 mL of 1:1 HCl and the minimum amount of distilled water were added and heated to dissolve completely and then it was increased to a volume of 1 L. To prepare the standard 0.01 M EDTA solution, 3.72 g of EDTA disodium salt was dissolved in water to a volume of 1 L. To standardize EDTA, 10 mL of standard calcium solution was poured into Erlenmeyer and 5 mL of pH = 10 buffer solution and 2 drops of ECBT indicator were added to produce a red color. Titration with EDTA solution was continued until the appearance of blue color and the volume of EDTA consumed was recorded and its exact concentration was subsequently calculated. In this study, in order to measure the total hardness of the samples, 50 or 100 mL of the sample was poured into a beaker and 5 mL of a buffer solution with pH = 10 and three drops of ECBT reagent were added to give a red color. The solution was then titrated with standardized EDTA (until blue color appeared). Calcium and magnesium ions were titrated and the total amount of these two cations was reported in mg/L of $CaCO_2$. These reagents and chemicals can be obtained from Hach Chemical Company and are described in Standard Methods for the examination of Water and Wastewater [4].

## 3. Findings

Experimental range and levels of independent factors have been shown in Table 1. The results of the regression coefficients and the multiple-way ANOVA coefficients of the proposed model for the TDS reduction are given in Tables 2 and 3, respectively. Also, the results related to the regression coefficients and the multiple-way ANOVA coefficients of the proposed model for the EC reduction are shown in Tables 4 and 5, respectively. The results of the regression coefficients and the multiple-way ANOVA coefficients of the proposed model for the TH are also given in Tables 6 and 7, respectively. In Table 8, the mean and standard deviation of the reduction of TDS, EC and TH in the presence of the MF force, in the presence of the MHD force and in the absence of the MF and MHD forces. The reduction efficiencies of the TDS, EC and TH in the presence of the

Table 2
Regression coefficients of proposed model for TDS reduction

| | Regression coefficient | Standard error | *T*-value | Pr. > *F* |
|---|---|---|---|---|
| Intercept | 0.6135932 | 0.3779010 | 1.6237 | 0.107204 |
| NaCl ($X_1$) | 0.0719118 | 0.0888309 | 0.8095 | 0.419894 |
| $CaCO_3$ ($X_2$) | 0.0092647 | 0.0888309 | 0.1043 | 0.917118 |
| $MgSO_4$ ($X_3$) | –0.0307353 | 0.0888309 | –0.3460 | 0.729982 |
| Flow rate ($X_4$) | 0.1154412 | 0.0888309 | 1.2996 | 0.196373 |
| Diameter ($X_5$) | –0.0995588 | 0.0888309 | –1.1208 | 0.264742 |
| Distance ($X_6$) | 0.0123529 | 0.0888309 | 0.1391 | 0.889647 |
| Magnetic flux density distance ($X_7$) | 0.0985294 | 0.0888309 | 1.1092 | 0.269687 |
| $CaCO_3$: diameter | –0.1873438 | 0.0915648 | –2.0460 | 0.043055 |
| $X_4^2$ | 0.5537850 | 0.1769420 | 3.1298 | 0.002222 |

Multiple *R*-squared: 0.2033; Adjusted *R*-squared: 0.1535

Table 3
ANOVA results for the response surface first-order model for TDS reduction

| Source | d.f.[a] | Sum of square | Mean square | *F*-value | Pr. > *F* |
|---|---|---|---|---|---|
| Model | 7 | 17.130 | 2.4471 | 2.2802 | 0.0328001 |
| Residual | 144 | 122.341 | 1.0732 | | |
| Lack of fit | 107 | 117.833 | 1.1012 | 1.7101 | 0.2329521 |
| Pure error | 7 | 4.508 | 0.6439 | | |

[a]Degree of freedom

Table 4
Regression coefficients of proposed model for EC reduction

| | Regression coefficient | Standard error | *T*-value | Pr. > *F* |
|---|---|---|---|---|
| Intercept | 3.166471 | 0.829865 | 3.8156 | 0.0002021 |
| NaCl ($X_1$) | –0.319559 | 0.414933 | –0.7701 | 0.4424925 |
| $CaCO_3$ ($X_2$) | –0.041765 | 0.414933 | –0.1007 | 0.9199670 |
| $MgSO_4$ ($X_3$) | –0.623824 | 0.414933 | –1.5034 | 0.1349481 |
| Flow rate ($X_4$) | –0.139559 | 0.414933 | –0.3363 | 0.7371103 |
| Diameter ($X_5$) | –0.325735 | 0.414933 | –0.7850 | 0.4337427 |
| Distance ($X_6$) | 0.511029 | 0.414933 | 1.2316 | 0.2201357 |
| Magnetic flux density distance ($X_7$) | 0.363824 | 0.414933 | 0.8768 | 0.3820624 |
| $X_3^2$ | 3.329673 | 0.757944 | 4.3930 | 2.154e-05 |
| $X_5^2$ | –1.676577 | 0.757944 | –2.2120 | 0.0285416 |

Multiple *R*-squared: 0.5776; Adjusted *R*-squared: 0.5359

Table 5
ANOVA results for the response surface first-order model for free EC reduction

| Source | d.f.[a] | Sum of square | Mean square | *F*-value | Pr. > *F* |
|---|---|---|---|---|---|
| Model | 4 | 272.94 | 68.234 | 2.7330 | 0.03209 |
| Residual | 121 | 3,020.97 | 24.967 | | |
| Lack of fit | 114 | 2,922.63 | 25.637 | 1.8249 | 0.20364 |
| Pure error | 7 | 98.34 | 14.048 | | |

[a]Degree of freedom

Table 6
Regression coefficients of proposed model for TH reduction

| | Regression coefficient | Standard error | *T*-value | Pr. > *F* |
|---|---|---|---|---|
| Intercept | 13.955588 | 0.873388 | 15.9787 | <2.2e-16 |
| NaCl ($X_1$) | –0.234853 | 0.436694 | –0.5378 | 0.59156 |
| $CaCO_3$ ($X_2$) | –0.843382 | 0.436694 | –1.9313 | 0.05544 |
| $MgSO_4$ ($X_3$) | –1.757941 | 0.436694 | –4.0256 | 9.211e-05 |
| Flow rate ($X_4$) | 0.097059 | 0.436694 | 0.2223 | 0.82443 |
| Diameter ($X_5$) | 0.328824 | 0.436694 | 0.7530 | 0.45271 |
| Distance ($X_6$) | –0.496324 | 0.436694 | –1.1365 | 0.25764 |
| Magnetic flux density distance ($X_7$) | –0.483529 | 0.436694 | –1.1072 | 0.27006 |
| $X_3^2$ | –0.52810 | 0.85363 | –0.6187 | 0.5371 |

Multiple *R*-squared: 0.4719; Adjusted *R*-squared: 0.431

MHD force were 4.64%, 26.26% and 21.64%, respectively. Furthermore, the reduction efficiencies of the TDS, EC and TH in the presence of the MP force were reported –1.63%, –3.51% and –3.04%, respectively (negative efficiency). The results of multiple-way ANOVA of variables at different levels of an independent variable type of force have been shown in Table 8. The RSM of the TDS reduction vs. NaCl concentration and $CaCO_3$ concentration is demonstrated in Fig. 1, and the RSM of the TDS reduction against NaCl concentration and $MgSO_4$ concentration is shown in Fig. 2 and also the RSM of the TDS reduction vs. NaCl concentration and magnetic flux density is depicted in Fig. 3. Moreover, the RSM of the EC reduction vs. NaCl concentration and $CaCO_3$ concentration is demonstrated in Fig. 4 and the RSM of the EC reduction against NaCl concentration and central discharge pipe diameter is shown in Fig. 5 and also the RSM of the EC reduction vs. $CaCO_3$ concentration and central discharge pipe diameter is depicted in Fig. 6. And finally, the RSM of the TH reduction as a function of $MgSO_4$ concentration and $CaCO_3$ concentration is given in Fig. 7. The adequacy of the proposed models was also assessed by the residual values against the fitted values. The plots related to residual values analysis of TDS, EC and TH models are given in Figs. 8–10, respectively. These include the plot of the residuals vs. fitted values, the normal Q-Q plot, the plot of the standard residuals against the fitted values,

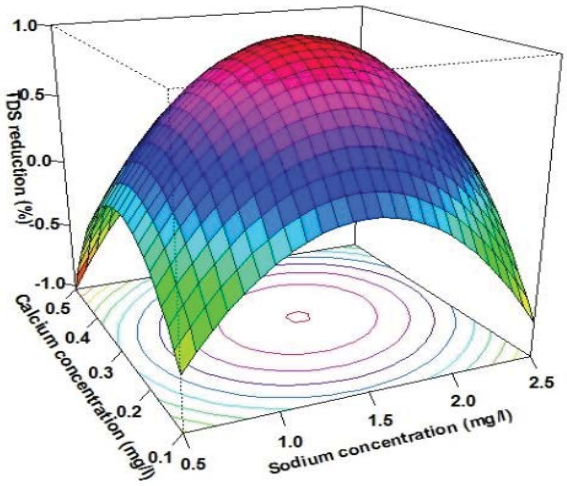


Fig. 2. Response surface for the TDS reduction as a function of NaCl and $CaCO_3$ concentrations.

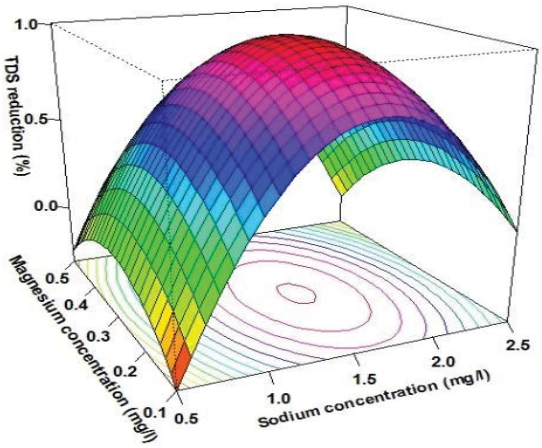


Fig. 3. Response surface for the TDS reduction as a function of NaCl and $MgSO_4$ concentrations.

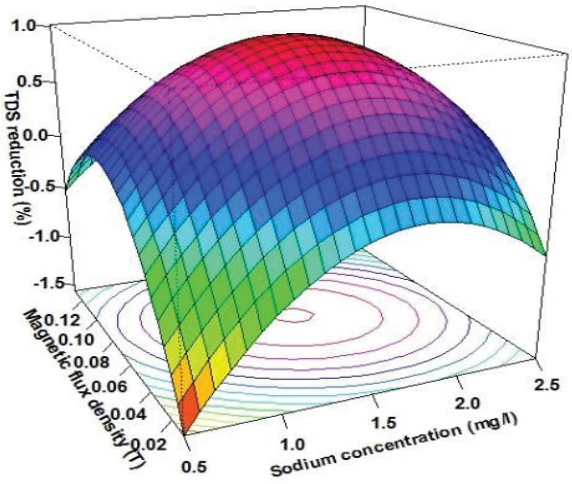


Fig. 4. Response surface for the TDS reduction as a function of NaCl concentration and magnetic flux density.

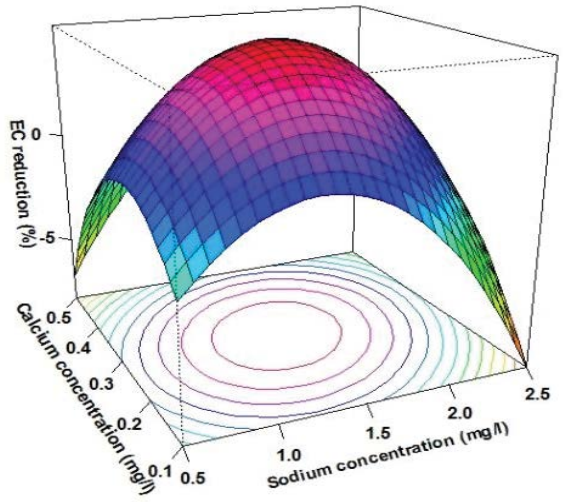


Fig. 5. Response surface for the EC reduction as a function of NaCl and $CaCO_3$ concentrations.

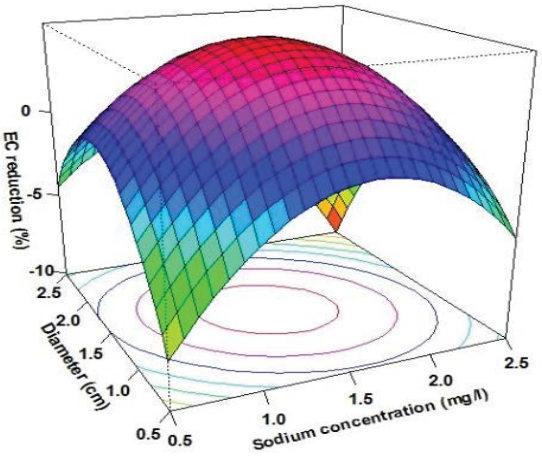


Fig. 6. Response surface for the EC reduction as a function of NaCl concentration and central tube diameter.

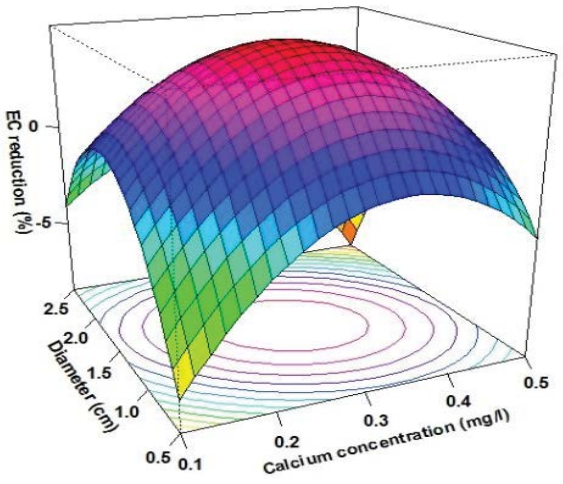


Fig. 7. Response surface for the EC reduction as a function of $CaCO_3$ concentration and central tube diameter.

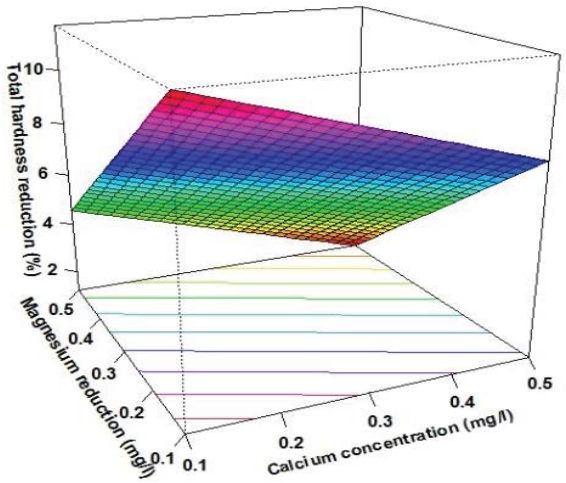


Fig. 8. Response surface for the TH reduction as a function of $CaCO_3$ and $MgSO_4$ concentrations.

and the residuals-leverage plot. In addition, the separate effect of each of these forces that were evaluated has been shown in Table 9. For this purpose, the sample that had the highest reduction of these three parameters was considered. In order to find the difference between the means, the data were analyzed at 3 levels of the force type using a multiple-way ANOVA test (Table 9). Figs. 11–13 also show the comparisons of the forces (MP and MHD) in the TDS, EC and TH reduction efficiencies, respectively. Moreover, the relationship between the magnetic flux density parameter and the TDS variable has been demonstrated in Fig. 14.

## 4. Discussion

### *4.1. TDS, EC and TH reduction by magnetic-electrochemical reactor*

In this study, the parameters of NaCl concentration ($X_1$), $CaCO_3$ concentration ($X_2$), $MgSO_4$ concentration ($X_3$), water flow rate ($X_4$), central drain pipe diameter ($X_5$), central pipe-electrode distance ($X_6$) and the magnetic flux density ($X_7$) were studied. The results of the study indicated that the desalination system was able to reduce the parameters of TDS, EC and TH. The results showed that the highest reduction efficiency of TDS was 7.64% that occurred at NaCl 1 g/L, $CaCO_3$ 0.3 g/L, $MgSO_4$ 0.3 g/L, outlet water flow rate 10 mL/s, central pipe diameter 0.5 cm, central tube-electrode distance 2.5 cm and magnetic flux density T 0.07, the highest reduction efficiency of EC was 38.32% that was reported at NaCl 1 g/L, $CaCO_3$ 0.3 g/L, $MgSO_4$ 0.1 g/L, flow rate 6 mL/s, central tube diameter 1.5 cm, central pipe-electrode distance 2.5 cm and magnetic flux density T 0.07, and the highest reduction efficiency of TH was 36.04% that was achieved at NaCl 2 g/L, $CaCO_3$ 0.2 g/L, $MgSO_4$ 0.2 g/L,

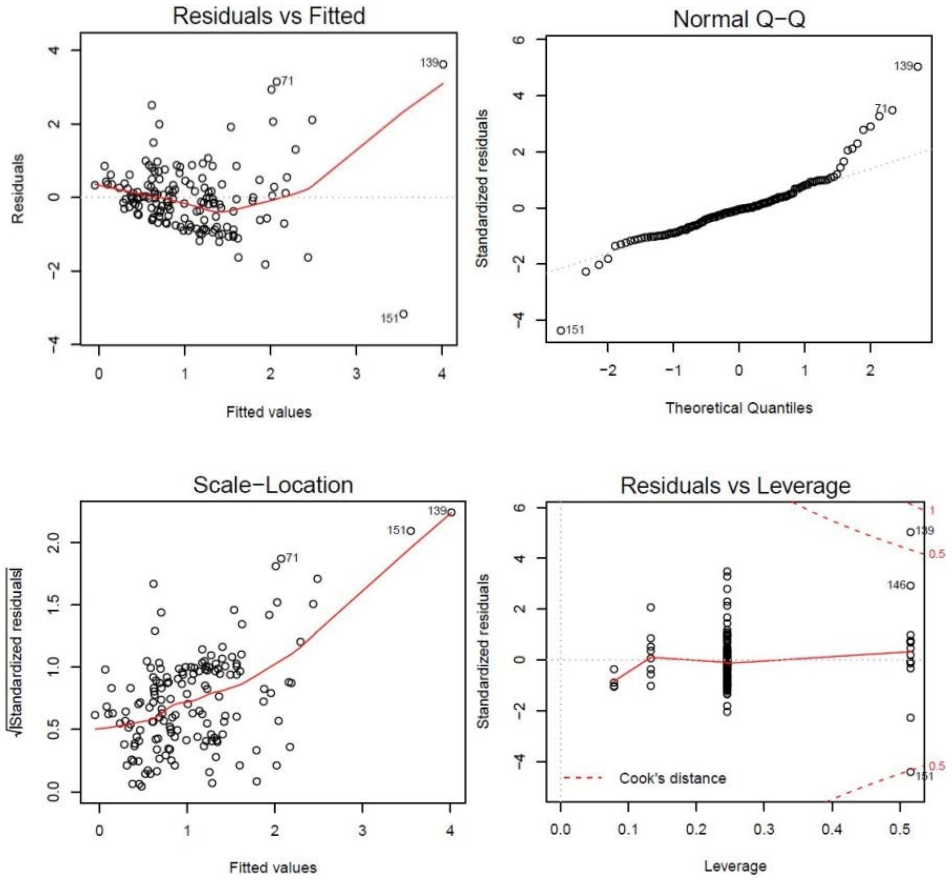


Fig. 9. The residuals plots related to the results of the response surface first-order model for TDS reduction.

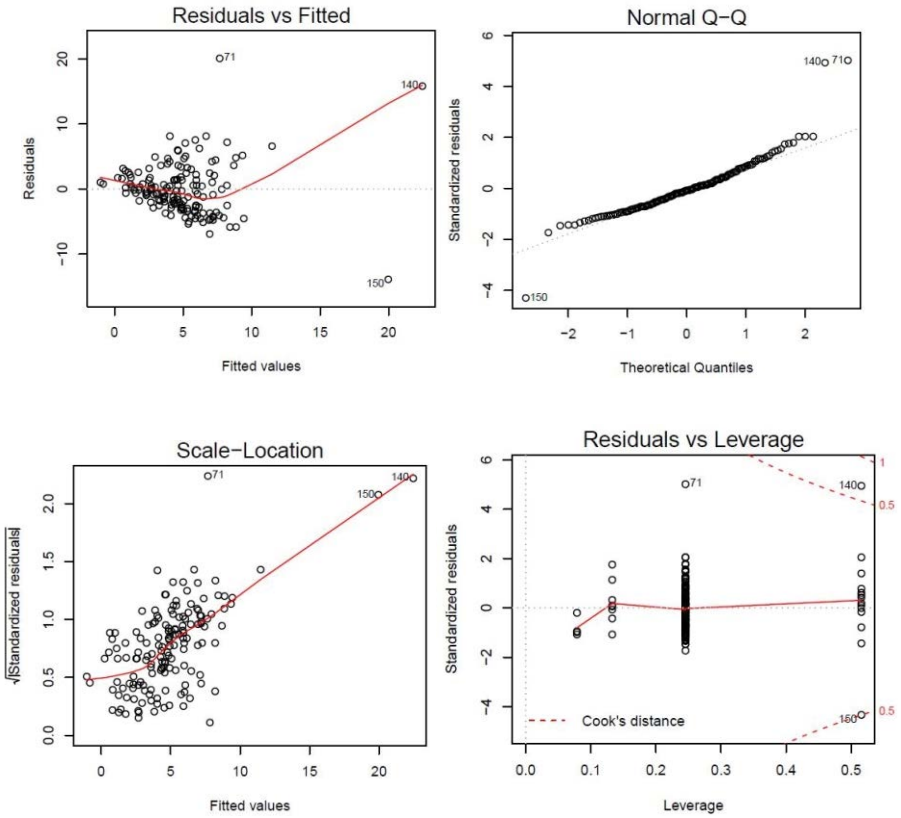


Fig. 10. The residuals plots related to the results of the response surface first-order model for EC reduction.

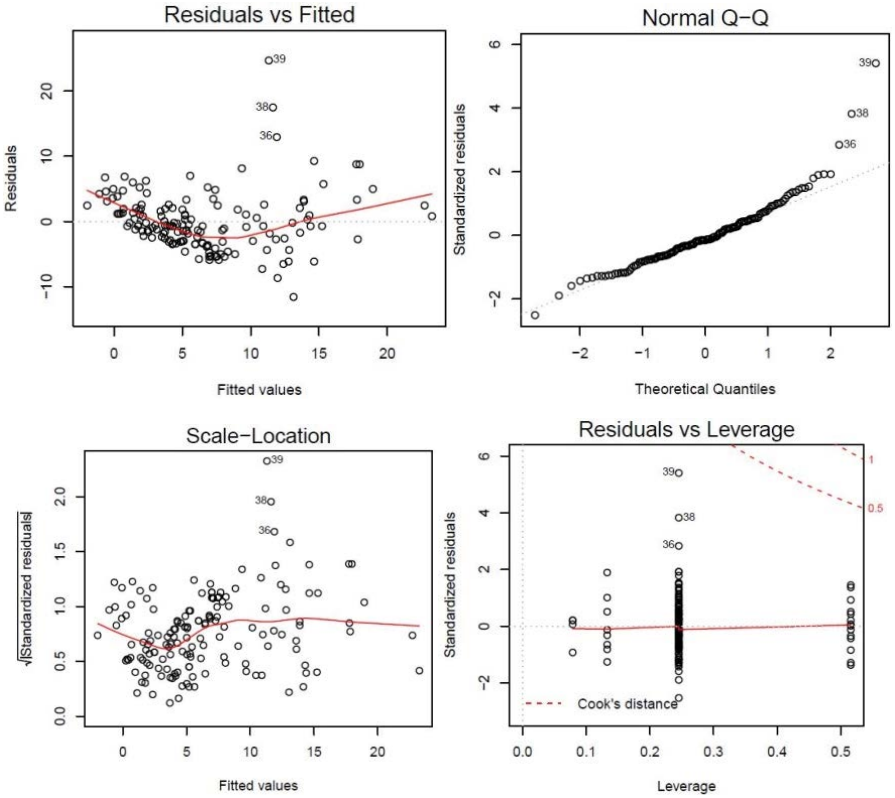


Fig. 11. The residuals plots related to the results of the response surface first-order model for TH reduction.

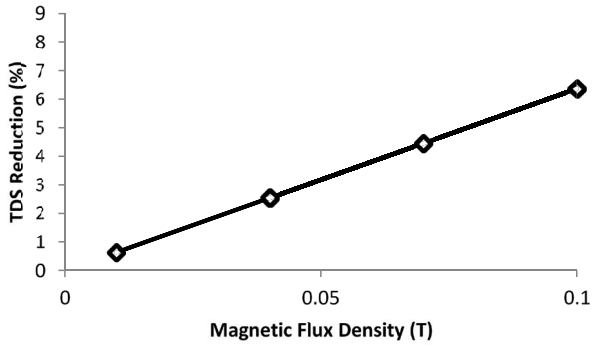


Fig. 12. Changes in the rate of reduction of TDS against changes in magnetic flux density.

effluent flow rate 4 mL/s, central tube diameter 1 cm, central pipe-electrode distance 2 cm and magnetic flux density T 0.04. The proposed model for TDS reduction was the quadratic model ($p$-value = 0.032) and the only statistically significant variable was the diameter of the central tube ($p$-value = 0.002) as shown in Table 2. Besides, the interaction between $CaCO_3$ concentration and the diameter of the central tube was significant ($p$-value = 0.043). The quality of the model was evaluated by the $R^2$ coefficient and lack of fit (LOF). The LOF value of the model (0.23) guaranteed a relatively good correlation between the predicted and experimental values because this value was higher than the considered significant level (0.05) (Table 3). Similarly, the EC reduction was based on the quadratic model ($p$-value = 0.032) and the $MgSO_4$ concentration and the diameter of the central tube were statistically significant ($p$-value = 0.00002 and $p$-value = 0.028) as shown in Table 4. The LOF value of the model (0.20) showed a relatively good correlation between the predicted and actual values (Table 5). Moreover, the proposed model for TH reduction was the first-order model ($p$-value = $4 \times 10^{-16}$) and the only statistically significant parameter was the $MgSO_4$ concentration ($p$-value = 0.00009) shown in Table 6. The LOF value of the model (0.63) showed a very good correlation between the predicted and actual values (Table 7). Moreover, the residual analysis diagrams of the TDS, EC and TH reduction models showed that the residual values were relatively well dispersed against the predicted values of the proposed model and did not follow a specific linear pattern. Also, the distribution of residual values was normal and was on the altered normal line (Figs. 10 and 11). The results of optimizing the response variables of this study showed that the stationary point or the optimal point of TDS was 1%, which was obtained in the sodium chloride of 1.56 g/L, calcium carbonate of 28.2 g/L, magnesium sulfate of 0.27 g/L, the water flow rate of 5.78 mL/s, the diameter of a central discharge tube of 1.61 cm, central pipe-electrode distance of 2.47 cm and magnetic flux density of 0.075 T (Figs. 2–4). Furthermore, the optimum point of EC was about 5% that was achieved at the sodium chloride of 1.49 g/L, calcium carbonate of 0.30 g/L, magnesium sulfate of 0.30 g/L, the water flow rate of 5.92 mL/s, the diameter of a central discharge tube of 1.41 cm, a central pipe-electrode distance of 2.31 cm and magnetic flux density of 0.11 T (Figs. 5–7). Finally, the optimal point (corresponding increment) of TH was about 12% that occurred at the sodium chloride of 0.05 g/L, calcium carbonate of 0.04 g/L, magnesium sulfate of 0.08 g/L, the water flow rate of 0.1 mL/s, the diameter of a central discharge tube of 0.07 cm, a central pipe-electrode distance of 0.11 cm and magnetic flux density of 0.006 T (Fig. 8). In this system, by MP and MHD forces, the first of which was generated by the electrolysis process and the second by the interaction of electric and magnetic forces, the laminar or plug flow of the existing ions changed, and the ions were directed in a conical direction and discharged into the central tube. Generally, an increase in TDS and EC in the effluent from the central tube shows the presence of more ions. Consequently, the presence of more ions in the central outlet water indicated that the ions were diverted to the central tube. Moreover, the ions of soluble salts were dissociated as a result of the process of electrolysis at the top of the column, resulting in a difference in ion concentration. The difference in the concentration of ions causes the formation of a concentration gradient. This gradient of ion concentration in magnetic fields creates a force called the Kelvin force [14]. This force is called the MP force. The reason for this naming is that this force is applied to the ions of an electrolyte that has a concentration gradient and is exposed to magnetic fields [14]. The electrolysis process was accelerated by the neodymium magnet around the electrodes. The generated magnetic fields accelerate the oxidation and reduction performed on the surface of the electrodes [15]. The reason for this is the acceleration of electrons or any electrically charged particle in the magnetic fields [15]. The study by Monzon and Coey [14] showed that electromagnetic forces are applied to electric currents and electrophoretic forces are applied to paramagnetic components. Their results also showed that the Kelvin force can occur due to both the gradient of magnetic fields and the gradient of paramagnetic components [14]. They conclude that in order to observe the Kelvin force, the magnetic field

Table 7
ANOVA results for the response surface first-order model for TH reduction

| Source | d.f.[a] | Sum of square | Mean square | $F$-value | Pr. > $F$ |
|---|---|---|---|---|---|
| Model | 4 | 2,685.7 | 671.42 | 25.8880 | $4 \times 10^{-16}$ |
| Residual | 142 | 3,682.8 | 25.94 | | |
| Lack of fit | 135 | 3,484.2 | 25.81 | 0.9093 | 0.633061 |
| Pure error | 7 | 198.7 | 28.38 | | |

[a]Degree of freedom

Table 8
Summary of recent MF water treatment studies on water minerals

| Solution | Magnetic flux density | Magnetic field effects | Ref. |
|---|---|---|---|
| Aggregating a commercial LUDOX silica sol with 36 nm primary particle size aggregated using $KNO_3$ solution to a size of 1,400 nm | 0.31 T | MF (Magnetic Fields) was efficient to disperse nanoparticles and intensify the dispersion process, especially under turbulent flow | [23] |
| | Permanent magnets NdFeB block magnet | Deaggregation effect was a combination of hydrodynamic forces and Lorentz forces | |
| $Ca^{2+}$ 318 mg/L; TH 540 mg/L as $CaCO_3$; TDS 690 mg/L | Solenoid coil | Increasing water velocity decreased MF efficiency | [24] |
| Conductivity 1,200 μS/cm | 0–100 V; 0–400 kHz | MF decreased conductivities by 17%–25% with different frequencies, whereas the untreated case dropped by 31% | [25] |
| | Solenoid coils | $CaCO_3$ particle size became smaller and the crystals were loose with MF | |
| 500 mg/L $CaCO_3$ | 0.16 T | Increasing MF treatment time had negligible effect<br>There was a maximum efficiency at an optimal flow rate 1 | [26] |
| Potable water: TH 373 mg/L as $CaCO_3$; $Ca^{2+}$ 117 mg/L; $Mg^{2+}$ 14.7 mg/L | 0.33 T | Suspended particles could be fragmented by MF at a turbulent flow | [27] |
| | NdFeB block magnet | No effect of deaggregation under laminar regime<br>Turbulent flow conditions were required for effective MF | |
| $Ca^{2+}$, $CO_3^{2-}$, and $HCO^{3-}$; 300–500 mg/L as $CaCO_3$ | 0.16 T | MF increased the total precipitates and favored the homogeneous nucleation<br>MF effects depended on flow rate and residence time | [28] |
| pH 6.4; alkalinity 16 mg/L; TDS 38 mg/L; EC 56 μS/cm | 0.05–0.2 T | EMF (Electromagnetic Fields) increased the solution content of $Mg^{2+}$, $K^+$, $Na^+$, $Cl^-$, alkaline and $SiO_2$, decreased $Ca^{2+}$ and $SO_4^{2-}$ | [10] |

MF is magnetic field, T is tesla (unit)

Table 9
Mean and standard deviation of TDS, EC and TH in the presence of the MF force, in the presence of the MHD force and in the absence of the MF and MHD forces

| | Without MHD and MF forces | MF force | MHD force |
|---|---|---|---|
| TDS | 0.00 ± 0.000 | –1.63 ± 0.250 | 4.64 ± 0.115 |
| EC | 0.00 ± 0.000 | –3.51 ± 0.156 | 4.64 ± 0.115 |
| TH | 0.00 ± 0.000 | –3.04 ± 0.684 | 4.64 ± 0.115 |

gradient and the paramagnetic particle concentration gradient should not be aligned. The Kelvin force can increase due to the presence of ferromagnetic elements and the formation of concentration gradients [14]. The MHD was generated by the coil around the column and the central electrode [29]. The mechanism of coil interaction with the central electrode is similar to that of an electric motor. There are two windings in an electric motor. There is a coil in the center of the motor called the rotor and a coil around the rotor called the stator [6]. The electric current entering the stator causes magnetic field lines to form between the sides of the stator. When an electric current enters the central winding (rotor), an interaction occurs between the two windings [6]. If a wire is placed between two magnets with opposite poles so that the wire is perpendicular to the lines of the magnetic field and an electric current is applied to the wire, a force is applied to the wire by magnetic fields, which is perpendicular to the wire. This force is called the Laplace force [30]. In this study, the coil around the column acts as the stator and the center electrode of the column through which direct current flow passes through the rotor. As current flows through the coil, the movement of electrons inside the coil creates magnetic fields around it. Half of this field, which is perpendicular to the direction of the electric current of the coil and aligned with the central electrode, passes through the center of the column [29]. By applying a direct electric current to the central electrode, a force similar to that of the wire described above is applied to the electrode, but the electrode is fixed in the center of the tube and cannot move. However, this lack of movement of the central electrode, which acts as a rotor in the electric motor, does not mean that no force is applied [6]. The interaction of the coil and the central electrode creates force vectors around the central electrode that form circular paths that are not visible. There is water around the electrode inside the column. The water in the column contains mineral salts. Mineral salts dissolve in water and form ions,

which are called electrolyte solutions [31]. Electrolytes can conduct electricity through these ions. This type of conductor is called an ionic conductor [32]. The electric charge is transferred through ions from one electrode to another [33]. The ions in the electrolyte around the electrode are affected by the force vectors and are placed along the circular paths of the force or fields and begin to move [19]. According to the law of electromagnetic induction, electric fields can produce magnetic fields and magnetic fields can also create electric fields [34]. The magnetic fields generated by the coil passing through the center of the tube form electric fields around it [35]. The ions in solution, when beginning to move in the direction of the electric fields formed around the magnetic lines, intersect the magnetic field lines formed by the coil that passes vertically through the coil [19]. Based on Lorentz theory, whenever a charged particle is placed in magnetic and electric fields that are perpendicular to each other, the particle exerts a force perpendicular to the lines of both types of field, called the Lorentz force, which is the Laplace force applied to the wire [36]. Table 8 summarizes the details of recent MF water treatment including the feed water solution, MF devices and magnetic flux density, materials and operating conditions, characterization methods and major results. This table only shows the effect of magnetic fields because the simultaneous effect of magnetic and electric fields has not been studied in previous studies. As shown in the table, Han et al. [10] decreased $Ca^{2+}$ and $SO_4^{2-}$ from synthetic brine solution at the magnetic field of 0.05 to 0.2 T. The relationship between the magnetic flux density and the TDS reduction is shown in Fig. 12. According to the figure, the TDS removal efficiency increased with increasing magnetic flux density (due to increasing electric current intensity). This was due to the smaller Larmore radius (diameter of the spiral path of the particle), which caused more ions to discharge through the central tube. In other words, as the intensity of the electric current increased, more ions were directed to the central discharge tube, and as a result of this increase, the Larmore radius became smaller. Terentiev et al. [19] showed that differences in the concentration of ions in water exposed to non-uniform magnetic fields give rise to a spiral current called Larmore. Also, they optimized the diameter of the Larmore discharge radius of mineral components in a magnetic system by changing the current intensity. They found that when the electric current was between 0.03 and 0.1 Å, the Larmore radius increased, but when the electric current increased to 0.1 Å, the Larmore radius became smaller and more ions left the tube, which confirmed the results of this study [19]. They also reported that when the current intensity of the coil increased from 0.18 to 0.38 A, the Larmore radius of rotation of the ions decreased from 24 to 7 cm [19]. Monzon and Coey [13] reported in a review study that studies of the effect of magnetic fields on electric current focused on hydrodynamic magnetic currents. Their results also show that flow control on a millimeter-scale may be performed using an external magnetic field with paramagnetic components in a water sample [14]. From their study, it was concluded that the interaction of the magnetic field with the current density causes water to rotate around the electrode, which is called the MHD force and occurs in uniform magnetic fields. They reported that the protrusions on the cathode surface, which can occur due to non-uniform deposition, cause micro hydrodynamic currents around the protrusions [13]. Moreover, as the magnetic fields in the center of the coil get closer to each other, ions are applied more force as they move downward, and the diameter of the electric fields becomes smaller. The radius of these fields is called the Larmore radius, which can be calculated [19]. The Larmore radius is directly proportional to the mass and velocity of the particle and is inversely related to magnetic flux density. Therefore, the ions around the central electrode follow a spiral path. The Larmore radius in the center of the coil became zero and again began to enlarge as the distance between the magnetic fields opened [19]. In this study, the highest removal efficiency of TDS and EC was obtained at the diameter of the central tube of 1.5 cm and the central tube-electrode distance of 2.5 cm. Besides, the highest TH removal efficiency was obtained in the diameter of the central tube 1 cm and the central tube-electrode distance of 2 cm. These results indicate that ions that increase the TDS and EC of water (such as NaCl and $MgSO_4$) have a larger rotation diameter or Larmore radius than ions that increase water TH ($CaCO_3$).

### 4.2. Effects of MP and MHD forces

The MP force was created by the electrolysis process, which eliminated the effect of this force by cutting off the electric current between the two electrodes. The MHD force was also generated by the interaction of magnetic and electric fields. Each of these forces was separately considered. The mean and standard deviation of TDS, EC and TH in the presence of the MF force, in the presence of the MHD force and in the absence of the MF and MHD forces has been shown in Table 9. According to the table, the MHD force alone could reduce the TDS, EC and TH by 4.64%, 26.26% and 21.64%, respectively. Also, the MP force alone increased the TDS, EC and TH, which increased by 1.63%, 3.51% and 3.04%, respectively (negative efficiency). The results of multiple-way ANOVA of variables at different levels of the type of force have been given in Table 10. This small increase in these parameters (negative efficiency) was due to the generated ions around the electrodes that were discharged along with the treated stream. Had no effect on the reduction of TDS, EC and TH in the absence of these forces (Figs. 13–15). The results of statistical analysis of the difference between the means at different levels of the independent force factor showed that this difference was significant and the absence of any of the forces had an effect on the reduction of TDS, EC and TH. The greatest effect occurred when these two forces were applied simultaneously.

### 4.3. Effects of the oxygen atoms on salinity and hardness reduction

The results of this study also showed that calcium carbonate and magnesium sulfate salts had the greatest effect on reducing TDS, EC and TH among the studied salts. The effect of $MgSO_4$ was greater than that of $CaCO_3$. The salts used in this study dissociate in water and form multi-atomic ions. There is no oxygen atom in the chemical composition of NaCl, but there are 3 oxygen atoms in the chemical composition of $CaCO_3$ and 4 oxygen atoms in the $MgSO_4$. One of the reasons that can justify this effect is the presence of more

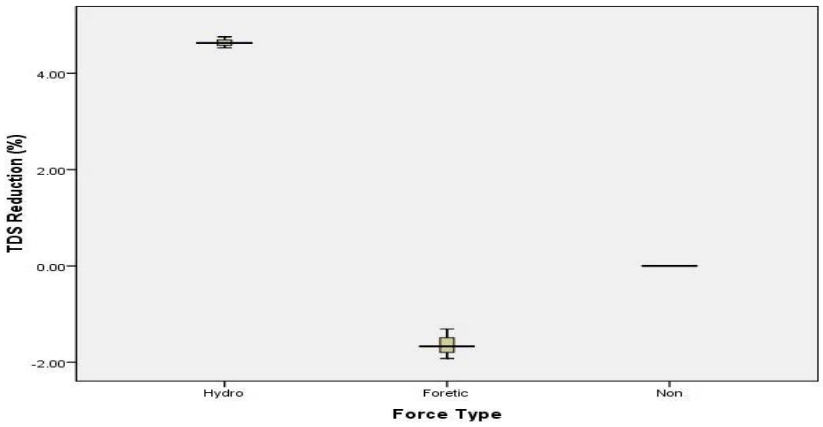


Fig. 13. Comparison of the mean of TDS against the force type.

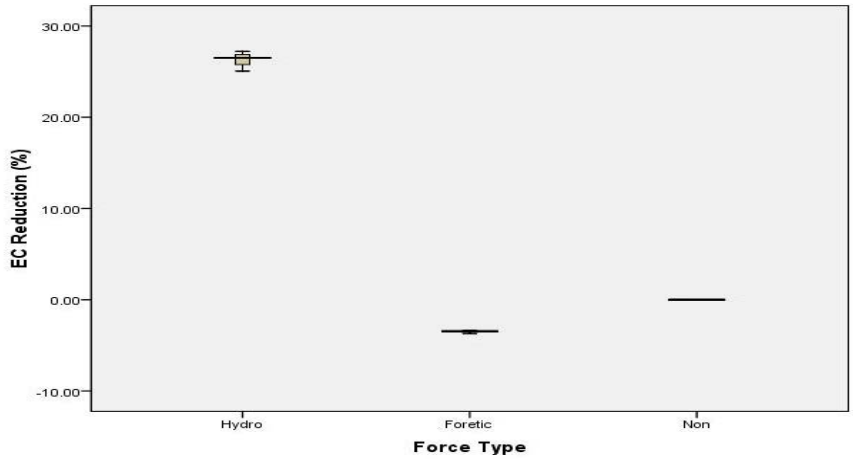


Fig. 14. Comparison of average EC against the force type.

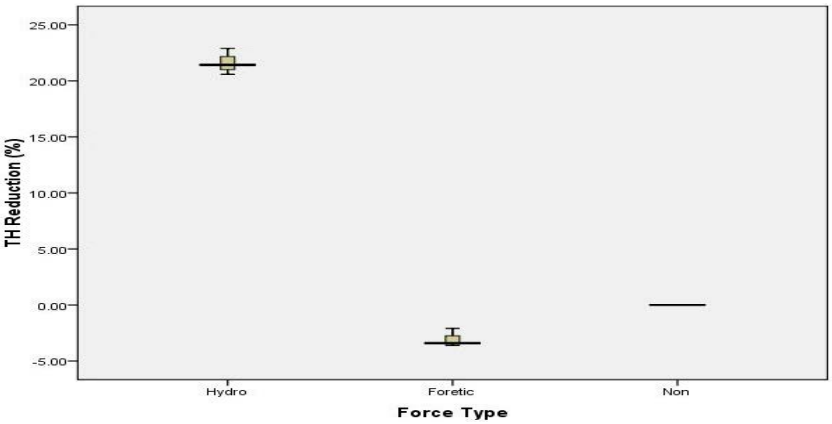


Fig. 15. Comparison of average TH against the force type.

oxygen atoms in the composition of $MgSO_4$. Therefore, the most effective variable in the interaction of magnetic and electrical forces and the conduction of water mineral components in a spiral flow around the central electrode was the presence of $MgSO_4$ salt and with less effect $CaCO_3$. The oxygen molecule has a paramagnetic property due to the presence of two unpaired electrons in the orbitals of the last layer of oxygen [37]. Paramagnetic is a form of the magnetic property of materials such as certain chemical elements and compounds. Paramagnetic materials have a relative magnetic permeability greater than or equal to one and are therefore slightly absorbed by the magnetic field. After removing the field,

Table 10
Results of multiple-way ANOVA of variables at different levels of independent variable type of force

| | Sum of squares | df | Mean square | *F* | Sig. |
|---|---|---|---|---|---|
| TDS* Force Between Groups (combined) | 63.552 | 2 | 31.776 | 888.150 | 0.000 |
| Within Groups | 0.215 | 6 | | | |
| Total | 63.767 | 8 | 0.036 | | |
| EC* Force Between Groups (combined) | 1,588.604 | 2 | 794.302 | 1.890E3 | 0.000 |
| Within Groups | 2.521 | 6 | | | |
| Total | 591.126 | 8 | 0.420 | | |
| TH* Force Between Groups (combined) | 1,086.942 | 2 | 453.471 | 782.711 | 0.000 |
| Within Groups | 4.166 | 6 | | | |
| Total | 1,091.108 | 8 | 0.694 | | |

*Mean difference is significant at the 0.05 level.

they do not retain their magnetic state because by removal of the thermal motion causes the spins to randomize [38]. Not only do electrons orbit the nucleus in atomic orbits, but they also spin. This rotation creates a magnetic field whose direction is indicated by a spin. Unpaired electrons, when exposed to magnetic fields, are aligned with the field lines and increase the effect of the magnetic field [39]. The magnetism coefficient and magnetic properties of the ions and salts studied in this study are given in Table 11. As shown in this table, dissolved oxygen (or ionic oxygen) has the highest magnetic susceptibility (+7,699 × $10^{-6}$ $m^3$/mol). This property causes $MgSO_4$ and $CaCO_3$ ions to be considered strong paramagnetic particles. And since there are more oxygen atoms in the composition of magnesium sulfate, the dissolved ion of this salt was more strongly affected by the magnetic field. Therefore, dissolved $MgSO_4$ ions should be placed in spiral paths around the central electrode for a shorter time and leave the central discharge tube with greater speed. Monzon and Coey [14] showed that the magnetic components in an electrolyte usually include paramagnetic cations, free radicals, and molecular species with unpaired spin, such as oxygen molecules. After experiments on the effect of a magnetic field on deionized water, Ozeki concluded that in the absence of air bubbles, the effect of a magnetic field was not observed even when electrolytes were added to pure water [40]. The results of the study showed that the effect of the magnetic field can be increased by the presence of oxygen and suggested that oxygen may be a dominant factor in the magnetic purification of water and it can be intentionally added to water. Brine water management is one of the most important problems in water desalination industries. The disposal of brine into the sea has adverse effects on the environment and marine life. Therefore, the development of this method for desalination of water can solve the serious problem of concentrated effluent in membrane systems. It is also cost-effective and environmentally friendly.

Table 11
Magnetic susceptibility and magnetic properties of studied salts and ions

| Salt/ion | Magnetic property | Magnetic susceptibility ($m^3$/mol) |
|---|---|---|
| NaCl | Diamagnetic | –30.2 × $10^{-6}$ |
| $Na^+$ | Paramagnetic | +16 × $10^{-6}$ |
| $Cl^-$ | Diamagnetic | –40.4 × $10^{-6}$ |
| $CaCO_3$ | Diamagnetic | –38.2 × $10^{-6}$ |
| $Ca^+$ | Paramagnetic | +40 × $10^{-6}$ |
| $MgSO_4$ | Diamagnetic | –135.7 × $10^{-6}$ |
| $Mg^+$ | Paramagnetic | +13.1 × $10^{-6}$ |
| $O^{2-}$ | Paramagnetic | +7,699 × $10^{-6}$ |

## 5. Conclusion

Due to the lack of sufficient methods to dispose of saline effluent produced during the desalination process, the use of a desalination system is limited. Salinity and hardness ions can be separated from the mainstream of water by the magnetic-electric desalination method. From the results of this study, it was concluded that the absence of any of the forces had a major effect on reducing the salinity and hardness of water and that the effect of the MHD force (negative effect) was greater than that of the MP force (positive effect). The greatest impact occurred when these two forces were applied simultaneously. Besides, the ions that increase the TDS and EC of water (such as NaCl and $MgSO_4$) have a larger rotation diameter or Larmore radius than ions that increase water TH. Furthermore, the most influential variable in the interaction of magnetic and electrical forces and the conduction of mineral components of water in a spiral flow was the presence of $MgSO_4$ and with less effect $CaCO_3$. This effect occurred as a result of the presence of oxygen atoms of $MgSO_4$ due to unpaired orbitals, which makes them more strongly affected by magnetic-electrical interactions. This system can be used to reduce condensed water in membrane technologies, and compared to other methods of deionization of water, this method does not require the addition of chemicals, it is easy to operate and use, and also it consumes very little energy. This method is a new idea and requires more experimental studies in order to achieve greater efficiency.

## Conflicts of interest statement

The authors declare that they have no known competing financial interests or personal relationships that

could have appeared to influence the work reported in this paper.

**Acknowledgments**

This study was supported financially by the Institute for Environmental Research (IER), Tehran University of Medical Sciences (Grant number: 98-05-07-41868). The authors are grateful for the financial support provided by the mentioned center. Also, we appreciate the collaboration of the Department of Environmental Health Engineering Laboratories of the Tehran University of Medical Sciences.

**References**

[1] M. Sepehr, S.M.R. Fatemi, A. Danehkar, A.M. Moradi, Application of Delphi method in site selection of desalination plants, Global J. Environ. Sci. Manage., 3 (2017) 89, doi: 10.22034/gjesm.2017.03.01.009.
[2] I.J. Esfahani, J. Rashidi, P. Ifaei, C. Yoo, Efficient thermal desalination technologies with renewable energy systems: a state-of-the-art review, Korean J. Chem. Eng., 33 (2016) 351–387.
[3] A. Panagopoulos, K.-J. Haralambous, M. Loizidou, Desalination brine disposal methods and treatment technologies – a review, Sci. Total Environ., 693 (2019) 133545, doi: 10.1016/j.scitotenv.2019.07.351.
[4] R.B. Baird, Standard Methods for the Examination of Water and Wastewater, 23rd Water Environment Federation, American Public Health Association, American, 2017.
[5] F. Zarantonello, F. Mancin, R. Bonomi, Working in a team: development of a device for water hardness sensing based on an arduino–nanoparticle system, J. Chem. Educ., 97 (2020) 2025–2032.
[6] G. Ozair, J.T. Gutierrez, An overview of magnetic water treatment system & further course of study, J. Int. Environ. Appl. Sci., 5 (2010) 965–974.
[7] A. Yadollahpour, S. Rashidi, Z. Ghotbeddin, M. Jalilifar, Z. Rezaee, Electromagnetic fields for the treatments of wastewater: a review of applications and future opportunities, J. Pure Appl. Microbiol., 8 (2014) 3711–3719.
[8] C. Piyadasa, H.F. Ridgway, T.R. Yeager, M.B. Stewart, C. Pelekani, S.R. Gray, J.D. Orbell, The application of electromagnetic fields to the control of the scaling and biofouling of reverse osmosis membranes – a review, Desalination, 418 (2017) 19–34.
[9] Z. Eshaghi, M. Gholizadeh, The effect of magnetic field on the stability of (18-crown-6) complexes with potassium ion, Talanta, 64 (2004) 558–561.
[10] Y. Han, C. Zhang, L. Wu, Q. Zhang, L. Zhu, R. Zhao, Influence of alternating electromagnetic field and ultrasonic on calcium carbonate crystallization in the presence of magnesium ions, J. Cryst. Growth, 499 (2018) 67–76.
[11] E. Chibowski, A. Szcześ, Magnetic water treatment–a review of the latest approaches, Chemosphere, 203 (2018) 54–67.
[12] M.B. Miranzadeh, M. Naderi, H. Akbari, A. Mahvi, V. Past, Adsorption of arsenic from aqueous solutions by iron filings and the effect of magnetic field, Int. Arch. Health Sci., 3 (2016) 37–42.
[13] L.M.A. Monzon, J.M.D. Coey, Magnetic fields in electrochemistry: the Lorentz force. A mini-review, Electrochem. Commun., 42 (2014) 38–41.
[14] L.M. Monzon, J. Coey, Magnetic fields in electrochemistry: the Kelvin force. A mini-review, Electrochem. Commun., 42 (2014) 42–45.
[15] V. Gatard, J. Deseure, M. Chatenet, Use of magnetic fields in electrochemistry: a selected review, Curr. Opin. Electrochem., 23 (2020) 96–105.
[16] M.D. Pullins, K.M. Grant, H.S. White, Microscale confinement of paramagnetic molecules in magnetic field gradients surrounding ferromagnetic microelectrodes, J. Phys. Chem. B, 105 (2001) 8989–8994.
[17] J. Jang, S.S. Lee, Theoretical and experimental study of MHD (magnetohydrodynamic) micropump, Sens. Actuators, A, 80 (2000) 84–89.
[18] A. Szcześ, E. Chibowski, L. Hołysz, P. Rafalski, Effects of static magnetic field on water at kinetic condition, Chem. Eng. Process. Process Intensif., 50 (2011) 124–127.
[19] O. Terentiev, K. Tkachuk, O. Tverda, A. Kleshchov, Electromagnetic focusing of impurities in water purification, Eastern-Eur. J. Enterp. Technol., 4 (2016) 10–15.
[20] D. Fernandez, P. Maurer, M. Martine, J. Coey, M.E. Möbius, Bubble formation at a gas-evolving microelectrode, Langmuir, 30 (2014) 13065–13074.
[21] M. Naderi, S. Nasseri, Optimization of free chlorine, electric and current efficiency in an electrochemical reactor for water disinfection purposes by RSM, J. Environ. Health Sci. Eng., 18 (2020) 1343–1350.
[22] R.H. Myers, D.C. Montgomery, C.M. Anderson-Cook, Response Surface Methodology: Process and Product Optimization Using Designed Experiments, John Wiley & Sons, 2016, pp. 236–242.
[23] M. Rouina, H.-R. Kariminia, S.A. Mousavi, E. Shahryari, Effect of electromagnetic field on membrane fouling in reverse osmosis process, Desalination, 395 (2016) 41–45.
[24] K.A. Flack, M.P. Schultz, T.A. Shapiro, Experimental support for Townsend's Reynolds number similarity hypothesis on rough walls, Phys. Fluids, 17 (2005) 035102, doi: 10.1063/1.1843135.
[25] X.-k. Xing, C.-f. Ma, Y.-c. Chen, Z.-h. Wu, X.-r. Wang, Electromagnetic anti-fouling technology for prevention of scale, J. Central South Univ. Technol., 13 (2006) 68–74.
[26] C. Gabrielli, R. Jaouhari, G. Maurin, M. Keddam, Magnetic water treatment for scale prevention, Water Res., 35 (2001) 3249–3259.
[27] F. Alimi, M. Tlili, M.B. Amor, G. Maurin, C. Gabrielli, Effect of magnetic water treatment on calcium carbonate precipitation: influence of the pipe material, Chem. Eng. Process. Process Intensif., 48 (2009) 1327–1332.
[28] B. Stuyven, G. Vanbutsele, J. Nuyens, J. Vermant, J.A. Martens, Natural suspended particle fragmentation in magnetic scale prevention device, Chem. Eng. Sci., 64 (2009) 1904–1906.
[29] B. Mahmoud, M. Yosra, A. Nadia, Effects of magnetic treatment on scaling power of hard waters, Sep. Purif. Technol., 171 (2016) 88–92.
[30] T.N. Narasimhan, Laplace equation and Faraday's lines of force, Water Resour. Res., 44 (2008), doi: 10.1029/2007WR006221.
[31] M. Alimohammadi, M. Naderi, Effectiveness of ozone gas on airborne virus inactivation in enclosed spaces: a review study, Ozone: Sci. Eng., 43 (2021) 21–31.
[32] Y. Cao, T.G. Morrissey, E. Acome, S.I. Allec, B.M. Wong, C. Keplinger, C. Wang, A transparent, self-healing, highly stretchable ionic conductor, Adv. Mater., 29 (2017) 1605099, doi: 10.1002/adma.201605099.
[33] S. Gholami, M. Naderi, A.M. Moghaddam, Investigation of the survival of bacteria under the influence of supporting electrolytes KCl, CuI and NaBr in the electrochemical method, J. Res. Environ. Health, 4 (2018) 104–111.
[34] M.F. Iskander, Electromagnetic fields and Waves, Waveland Press, 2013, pp. 521–525.
[35] S. Gholami, M. Naderi, M. Yousefi, M.M. Arjmand, The electrochemical removal of bacteria from drinking water, Desal. Water Treat., 160 (2019) 110–115.
[36] M.B. Miranzadeh, M. Naderi, V. Past, The interaction effect of magnetism on arsenic and iron ions in water, Desal. Water Treat., 213 (2021) 343–347.
[37] S.I. Dikalov, Y.F. Polienko, I. Kirilyuk, Electron paramagnetic resonance measurements of reactive oxygen species by cyclic hydroxylamine spin probes, Antioxid. Redox Signaling, 28 (2018) 1433–1443.
[38] H.P.J. Wijn, Magnetic Properties of Metals: d-Elements, Alloys and Compounds, Springer Science & Business Media, 2012, pp. 100–108.
[39] R.D. Ambashta, M. Sillanpää, Water purification using magnetic assistance: a review, J. Hazard. Mater., 180 (2010) 38–49.
[40] S. Ozeki, I. Otsuka, Transient oxygen clathrate-like hydrate and water networks induced by magnetic fields, J. Phys. Chem. B, 110 (2006) 20067–20072.